

Supporting Information

Supramolecular Oscillation-Assisted Ion Transport in Solid Electrolytes

Yigui Xie^a, Weiran Zhang^{a*}, Luxue Zhang^a, Xuesong Liu^a, Guojian Yang^b, Yu-Mo Zhang^a and Sean Xiao-An Zhang^{a*}

^a *State Key Laboratory of Supramolecular Structure and Materials, College of Chemistry, Jilin University, Changchun, 130012, P. R. China*

^b *Smart Materials for Architecture Research Lab Innovation Center of Yangtze River Delta, Zhejiang University, Jiaxing, 314100, P. R. China*

* Corresponding authors.

E-mail addresses: seanzhang@jlu.edu.cn (S. X.-A. Zhang), zhangweiran@jlu.edu.cn (W. Zhang)

Supplementary Figures

Supplementary Figures 1 to 19

Supplementary Tables

Supplementary Table 1 to 3

Supplementary Methods

Supplementary Method 1: Materials and Methods

Supplementary Method 2: Synthesis of molecules

Supplementary Method 3: Preparation of the electrochromic devices

Supplementary Method 4: The shear strength test and load-bearing test of SPE-ECD

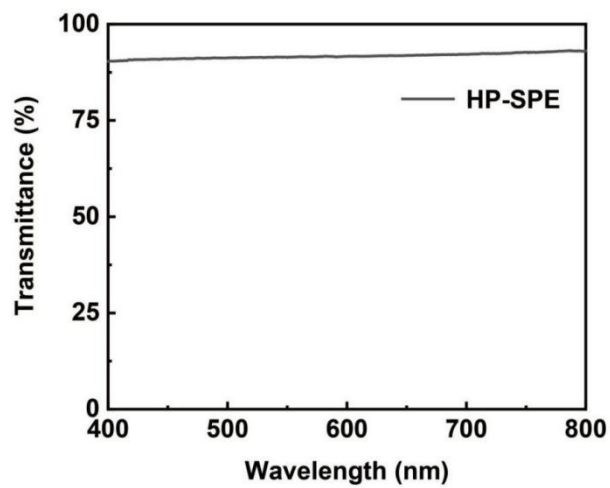
Supplementary Method 5: Determination of Solvent Residues by NMR Internal Standard Method

Supplementary Method 6: Investigation of the effect of air components on DMAc and DMAc-LiTFSI solution.

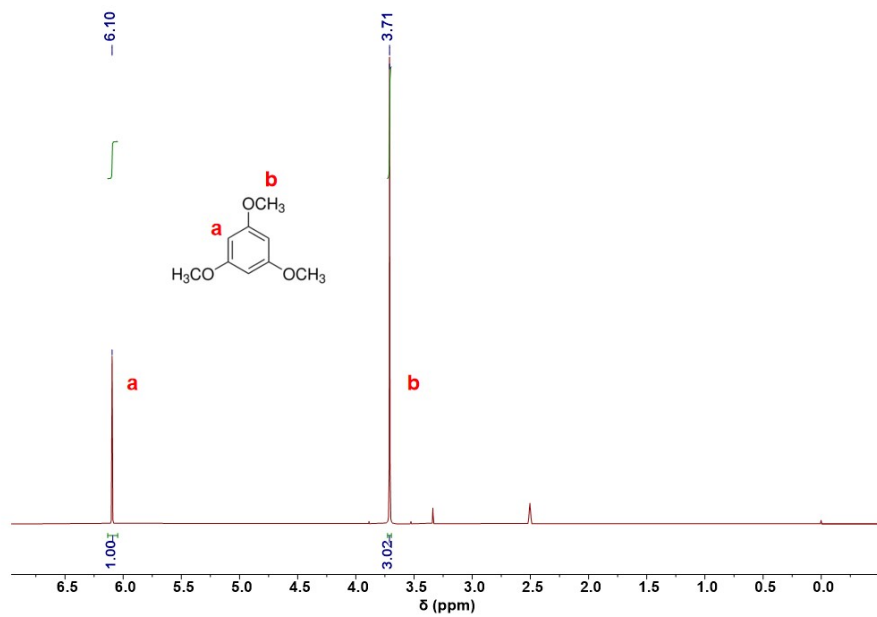
Supplementary Notes

Supplementary Note 1: Calculation of the Molar Ratio between DMAc and LiTFSI

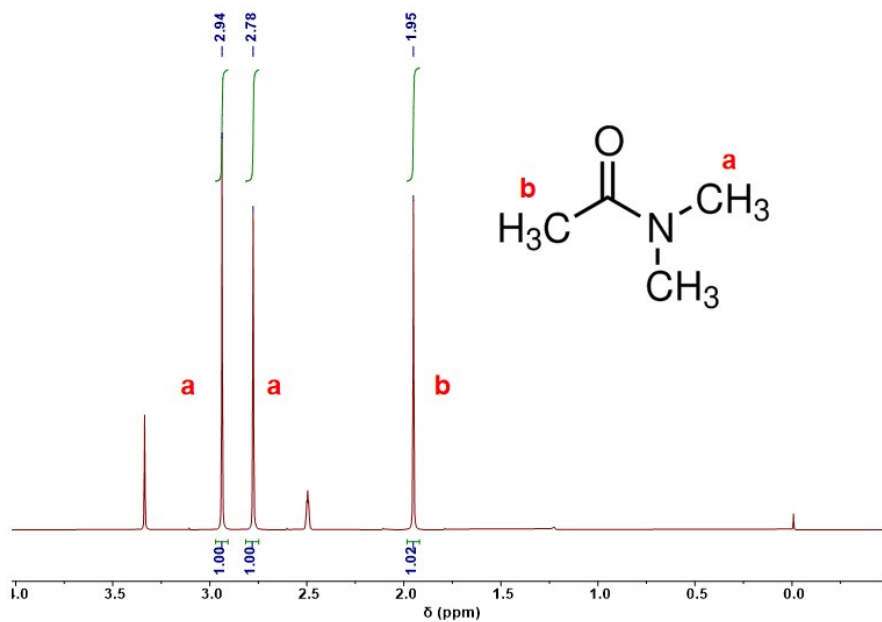
Supplementary References



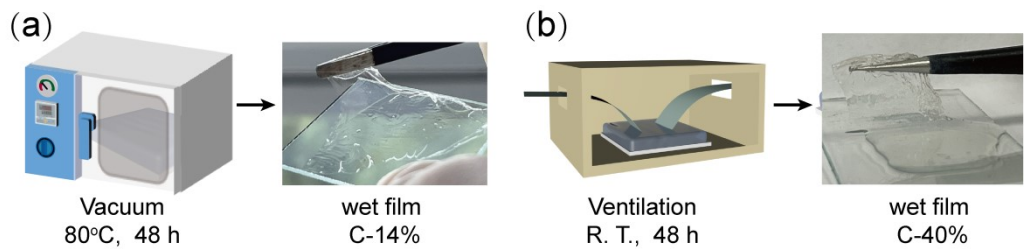
Supplementary Figure 1. Transmittance spectrum of HP-SPE between 400 and 800 nm.



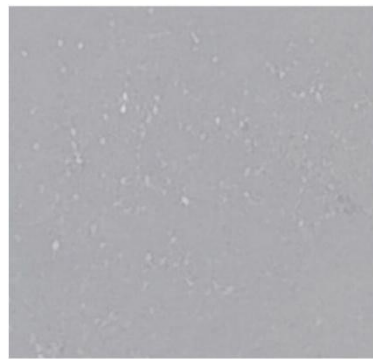
Supplementary Figure 2. ^1H NMR (400 MHz, $\text{DMSO-}d_6$) spectra of trimethoxybenzene.



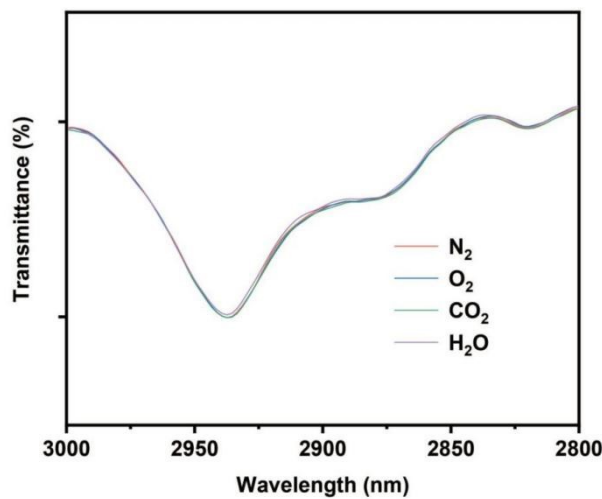
Supplementary Figure 3. ^1H NMR (400 MHz, $\text{DMSO}-d_6$) spectra of DMAc.



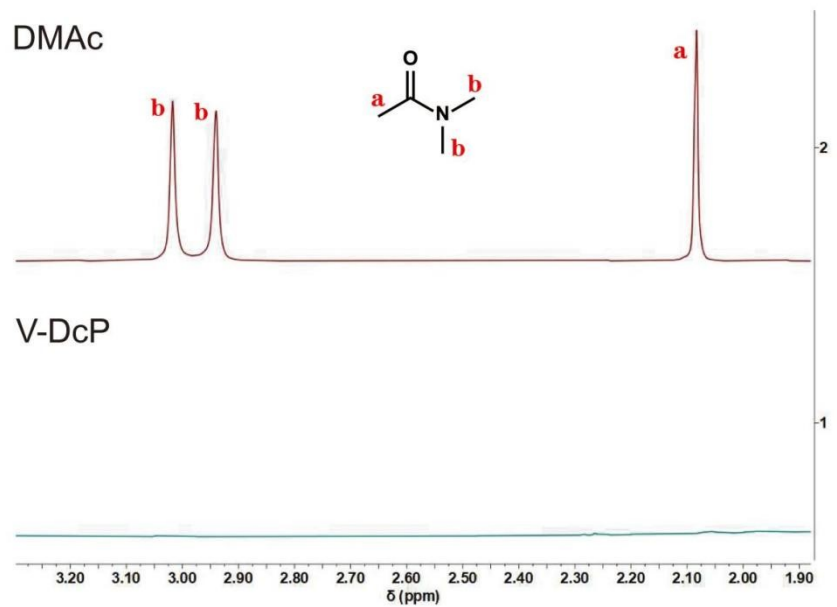
Supplementary Figure 4. (a) vacuum drying treatment and the physical photo of C-14%; (b) convection flow drying treatment and the physical photo of C-40%.



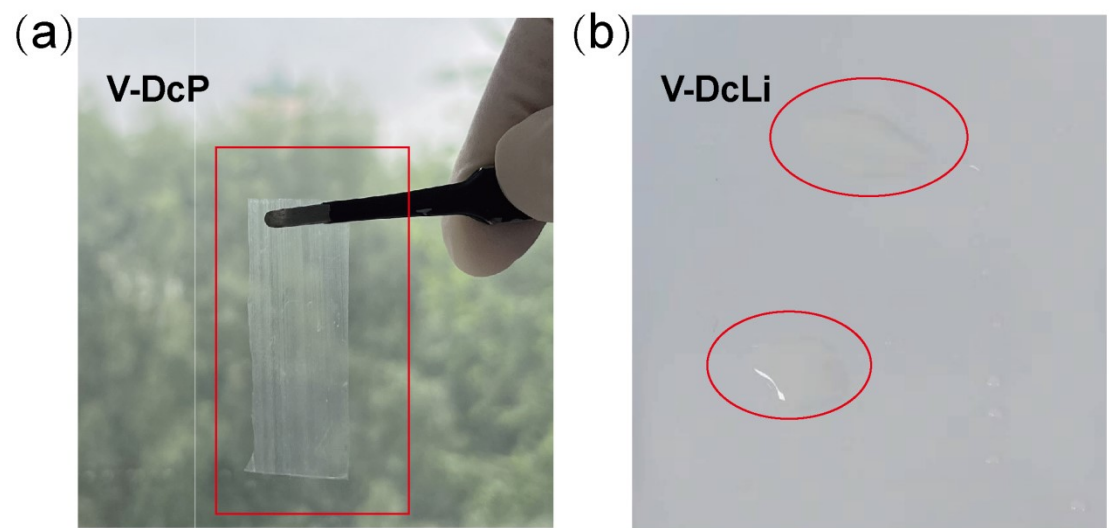
Supplementary Figure 5. The physical photo of the film after being dried in air for 48 hours. From the photo, it was clear that the film formed by this method was uneven and there was obvious precipitation.



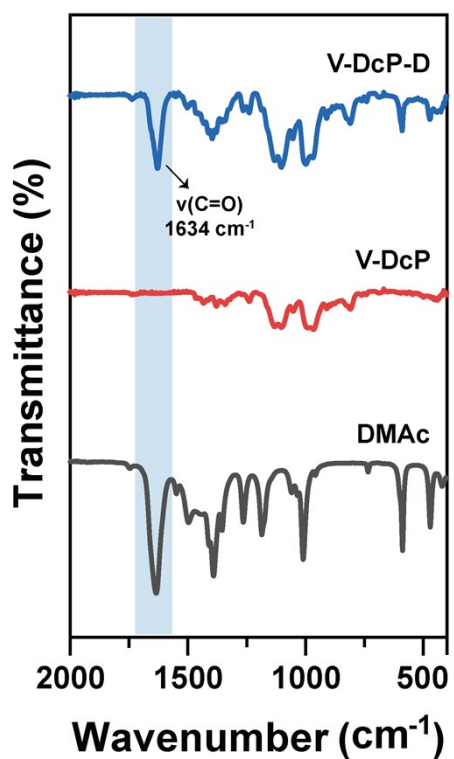
Supplementary Figure 6. Infrared spectra of the mixed solution of DMAc and LiTFSI before and after purging by different components in the air.



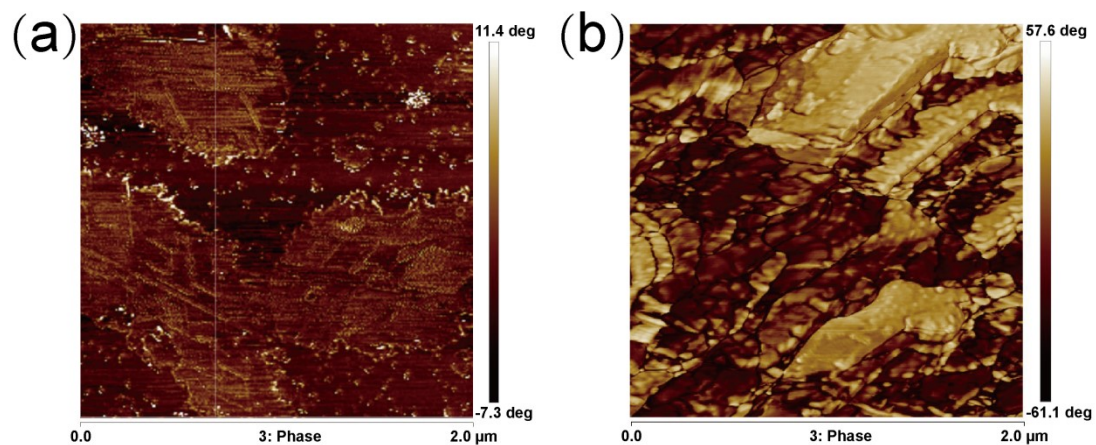
Supplementary Figure 7. ^1H NMR (400 MHz, $\text{CDCl}_3\text{-}d$) spectra comparison of DMAc and V-DcP.



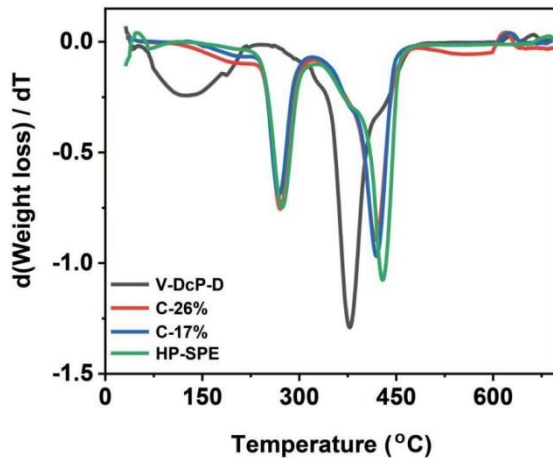
Supplementary Figure 8. Physical photos of (a) V-DcP and (b) V-DcLi.



Supplementary Figure 9. FT-IR spectra of DMAc, V-DcP and V-DcP-D.



Supplementary Figure 10. AFM images of (a) HP-SPE and (b) V-DcP.

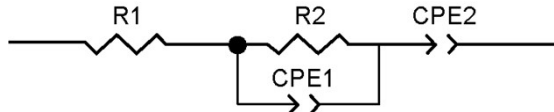


Supplementary Figure 11. The DTG curves of SPE and contrast membranes.

The thermal degradation behavior of the HP-SPE membranes was analyzed by thermogravimetric analysis (TGA), with the derivative thermogravimetry (DTG) curves presented here. The profiles exhibit two characteristic mass loss steps:

Step 1 (~250-350 °C): This initial decomposition step is observed only in the composites containing LiTFSI. It is assigned to the thermal decomposition of the lithium bis(trifluoromethanesulfonyl)imide (LiTFSI) salt, which is consistent with reported degradation onsets for LiTFSI in polymer matrices.^[1]

Step 2 (~400-500 °C): The second and predominant mass loss step corresponds to the decomposition of the polyvinyl butyral (PVB) polymer backbone.^[2] This step is present in all samples.



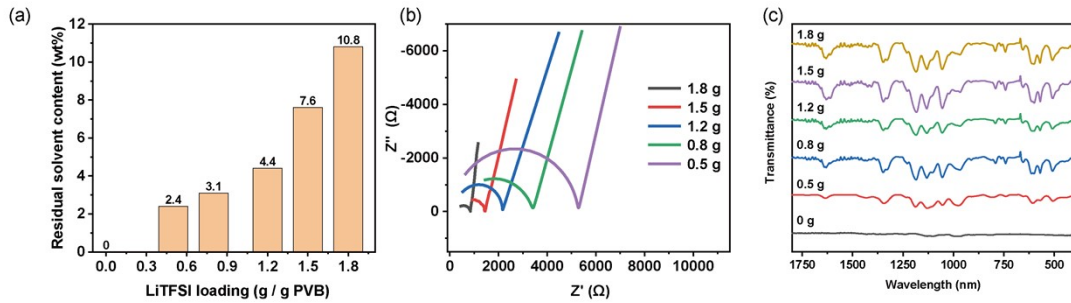
Supplementary Figure 12. Diagram of electrical components with impedance fitting. The bulk resistance (R_2) obtained from fitting was used to calculate the ionic conductivity.

R_1 represents the combined ohmic series resistance. It primarily includes the intrinsic bulk ionic resistance of the HP-SPE film itself. It is derived from the high-frequency intercept on the real axis of the Nyquist plot.

R_2 is the dominant resistive component associated with the ionic conduction process. In the context of our symmetric cell with blocking electrodes, it is most accurately described as the bulk resistance of the electrolyte. It quantifies the energy barrier for ion migration through the polymer matrix and is directly correlated with the diameter of the high-frequency semicircle.

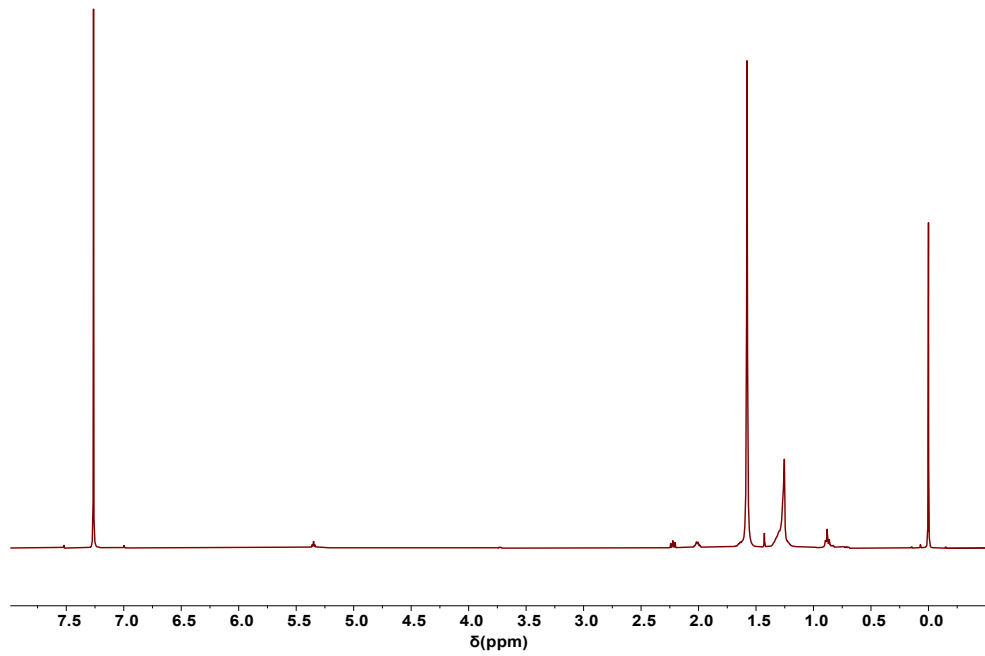
CPE1 accounts for the non-ideal capacitance of the electrochemical double layer.

CPE2 element describes the distributed, non-ideal diffusion or capacitive behavior at lower frequencies.

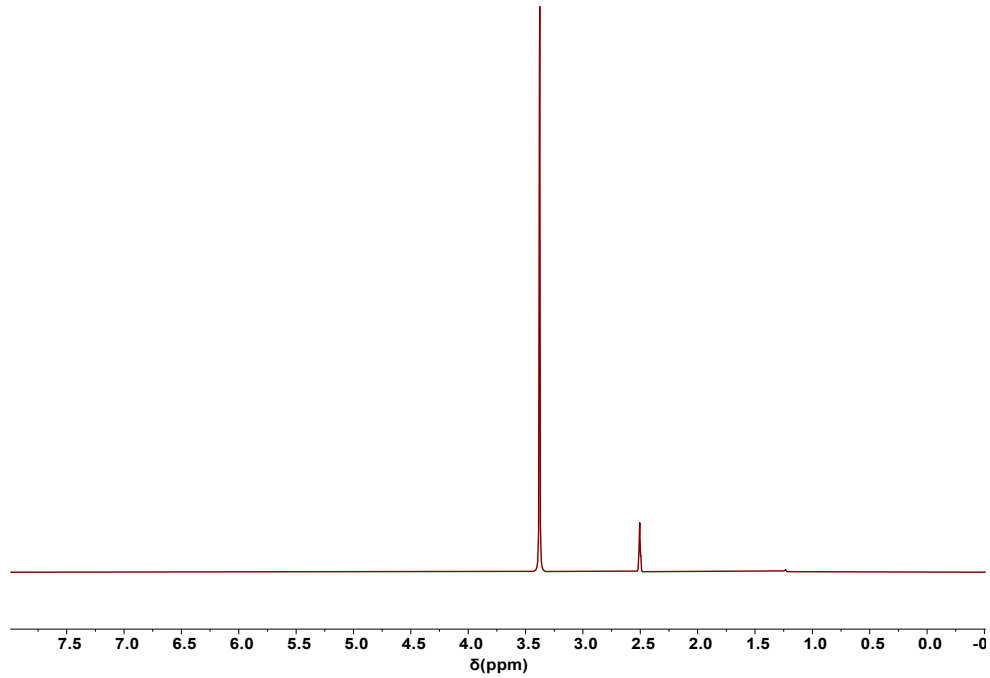


Supplementary Figure 13. (a) Residual DMAc content in HP-SPE membranes as a function of LiTFSI mass loading, determined by ^1H NMR; (b) Nyquist plots of HP-SPE membranes with varying LiTFSI content (per 1 g PVB), measured at 30 °C; (c) Stacked FTIR spectra of HP-SPE membranes with different LiTFSI loadings (per 1 g PVB).

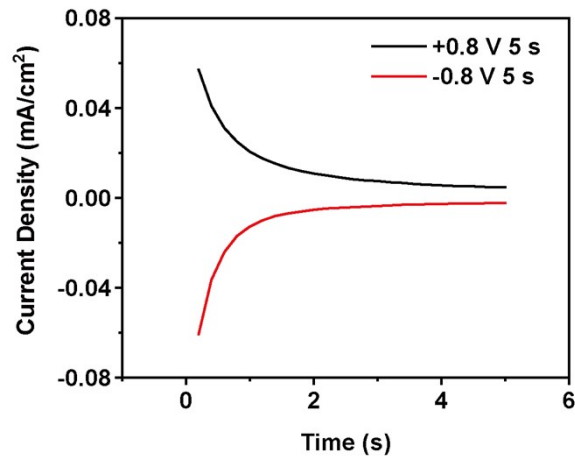
The residual DMAc content, quantified by ^1H NMR, increased monotonically with LiTFSI loading, confirming its crucial role in retaining the residual solvent via Li^+ –DMAc coordination. Concurrently, the bulk ionic resistance (at 30 °C) derived from electrochemical impedance spectroscopy exhibited a sharp decrease. The correlation between these two key parameters is summarized in Fig. 4e. The residual solvent content (essential for segmental mobility) and the bulk resistance (inversely related to conductivity) show opposing trends with increasing LiTFSI amount. The characteristic peak positions in the FTIR spectroscopy do not shift with concentration, indicating a similar local bonding environment once LiTFSI is introduced. This suggests that varying the LiTFSI concentration primarily changes the quantity of the conductive complex rather than its qualitative chemical nature.



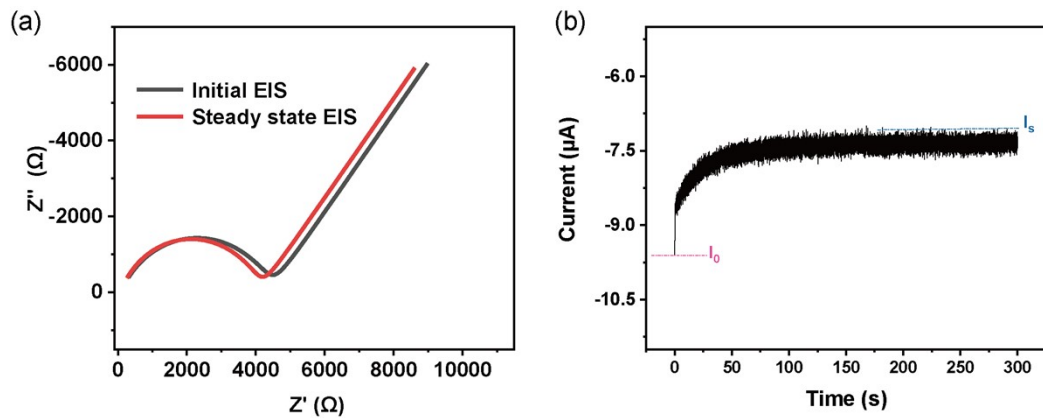
Supplementary Figure 14. ¹H NMR (400 MHz, Chloroform-*d*) spectra of Chloroform-*d* washed PBDF membrane. The solvent employed for the membrane preparation was DMSO.



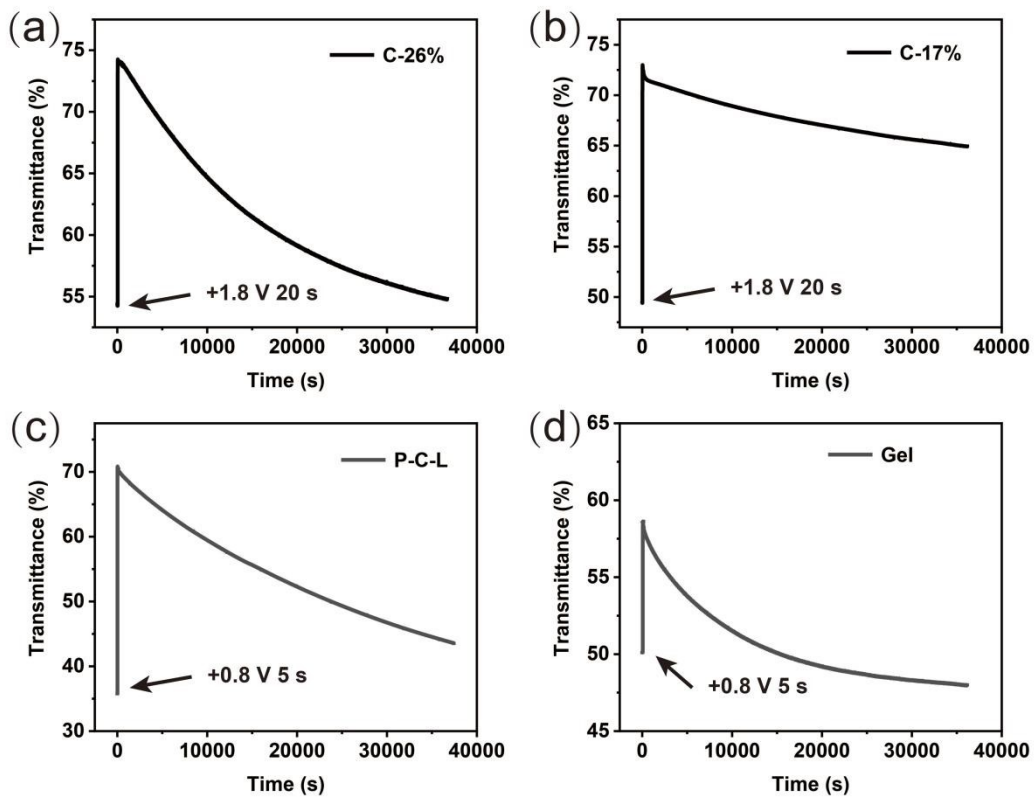
Supplementary Figure 15. ¹H NMR (400 MHz, DMSO-*d*₆) spectra of DMSO-*d*₆ washed 13001 membrane. The solvent employed for the membrane preparation was THF.



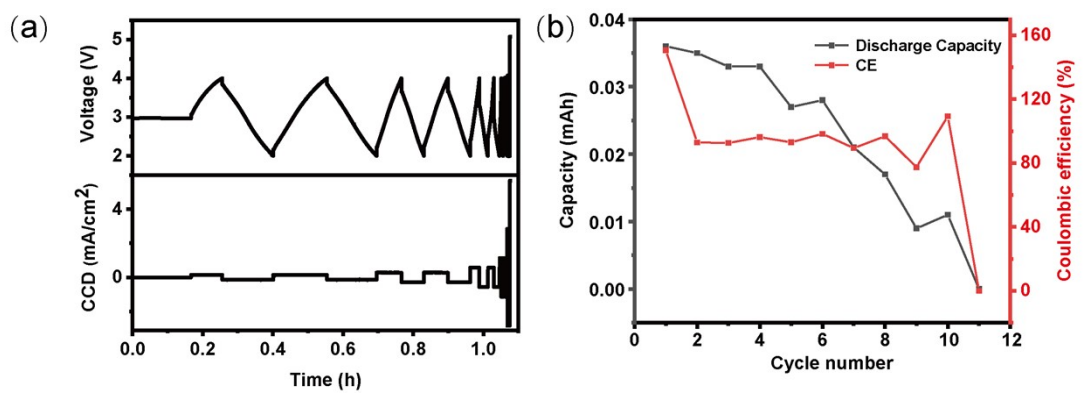
Supplementary Figure 16. Current density during electrical stimulation of the device.



Supplementary Figure 17. (a) Impedance of the SPE-ECD. The black curve is initial EIS before chronamperogram. The red curve is steady state EIS after chronamperogram. (b) Chronoamperogram of the SPE-ECD with an applied voltage of 10 mV. I_0 indicates the initial current, I_s means the steady state current.



Supplementary Figure 18. (a) Changes in transmission spectra at 600 nm during the stimulation of positive voltage (+1.8 V 20 s) then power off for the device made by C-26%; (b) Changes in transmission spectra at 600 nm during the stimulation of positive voltage (+1.8 V 20 s) then power off for the device made by C-17%; (c) Changes in transmission spectra at 600 nm during the stimulation of positive voltage (+0.8 V 5 s) then power off for the device made by P-C-L; (d) Changes in transmission spectra at 600 nm during the stimulation of positive voltage (+0.8 V 5 s) then power off for the device made by the gel film.



Supplementary Figure 19. Critical Current Density (CCD) test and initial cycling performance of an asymmetric Li | HP-SPE | AC cell.

Supplementary Table 1. Transference numbers of SPE-ECD.

	I ₀ (μA)	I _s (μA)	R ₀ (ohm)	R _s (ohm)	V(mV)	Transference Number (t +)
SPE-ECD	-9.53	-7.44	4316	4032	10	0.998

Supplementary Table 2. The Stability of the devices made by HP-SPE and the contrast electrolytes.

Electrolyte	Stability
HP-SPE	>160 h
Gel	10 min
P-C-L	50 min
C-26%	39 min
C-17%	94 min

Stability refers to the time it takes for the device spectrum to decay to 90% of the maximum ΔT after the power-off.

Supplementary Table 3. Comparison of ionic conductivity, optical contrast, switching time (coloration time and bleaching time), cycle stability and bistable time from previously reported electrochromic devices based on varying electrolytes.

State of Electrolytes	Ionic Conductivity (S/cm)	Optical Contrast ($\Delta T\%$)	Switching Time (s)	Cycle Stability (Cycles)	Bistable Time	Ref.
Solid	$\sim 10^{-5}$	$\sim 23\%$	$\sim 3.1/6.1$	~ 1000	>160 h	This work
Polymer membrane			(bleach/color)			

Solid	$\sim 10^{-4}$	$\sim 25\%$	$\sim 38.4/51.3$	~ 10000	>2000 s	[3]
Polymer membrane			(bleach/ color)			
Self supporting gel	$\sim 10^{-5}$	$\sim 41\%$	$\sim 10/10$	~ 1000	/	[4]
Polymer membrane			(bleach/ color)			
Inorganic ceramics	/	$\sim 53\%$	$\sim 33.4/62.5$	~ 500	/	[5]
			(bleach/ color)			
Polyionic liquid	$\sim 10^{-4}$	$\sim 36.3\%$	$\sim 20/30$	~ 5000	/	[6]
			(bleach/ color)			
Solid	$\sim 10^{-3}$	$\sim 85\%$	$\sim 3.2/3.0$	~ 10000	/	[7]
Polymer membrane			(bleach/ color)			

Supplementary Method 1. Materials and Methods

Materials

N,N-Dimethylacetamide (99.8%, Extra Dry, with molecular sieves, Water≤50 ppm (by K.F.), EnergySeal), 3,7-Dihydrobenzo[1,2-b:4,5-b']difuran-2,6-dione, (3-Glycidyloxypropyl)trimethoxysilane (KH560), Lithium Bis(trifluoromethanesulfonyl)imide (LiTFSI), 2,2-bimethoxy-2-phenylacetophenone (DMPA) and propylene carbonate (PC) were purchased from Energy Chemical. Polyvinyl butyrals (PVB) (M.W.40,000-70,000) were purchased from Shanghai Bide Pharmaceutical Technology Co., LTD. Polyethylene glycol diacrylate (average Mn 700, acrylate, 100 ppm MEHQ as inhibitor, 300 ppm BHT as inhibitor) were purchased from Sigma Aldrich (Shanghai) Trading Co., LTD. Poly(methyl methacrylate) (PMMA) were purchased from Sinopharm Chemical Reagent Co., Ltd. Copper(II) acetate (anhydrous, 97%) were purchased from Anhui Zesheng Technology Co., LTD. 13001 were purchased from Jilin Huazhen Science & Technology Company. Transparent indium tin oxide glass electrode (ITO) was purchased from CSG Holding Co., Ltd. Polytetrafluoroethylene film (3 μ m thick) were purchased from Shenzhen Xinzheyu Plastic Materials Business Department.

Instrument characterization

UV-Vis transmittance spectra were measured using a Shimadzu UV-2550 double-beam spectrophotometer. Current was obtained from Bio-logic electrochemical work station and IVIUM Vertex.C.EIS electrochemical workstation (Tianjin Brillante Technology Limited, China). Electrochemical impedance spectra were measured on IVIUM Vertex.C.EIS electrochemical workstation (Tianjin Brillante Technology Limited, China). Nuclear magnetic resonance spectra (1 H NMR) were recorded with Wuhan Zhongke Niujin As 400 (400 MHz for 1 H NMR and 101MHz for 13 C NMR). Chemical shift values were given relative to tetramethylsilane (TMS). Infrared (IR) spectra in the range of 4000 to 400 cm^{-1} were recorded using a vacuum Fourier Transform IR spectrometer VERTEX 80V-ATR. The thermal properties were measured using a thermogravimetric analyzer (Q500, TA) at a heating rate of 10 K/min. Raman spectra were recorded by grating type Raman spectrometer of HORIBA JOBIN YVON, France. Atomic Force Microscope

(AFM) images were taken in the tapping mode with a Nanoscope scanning probe microscope from Digital Instruments. Electrochemical cycling performance of the Li | HP-SPE | AC coin cells (15 mm in diameter) was evaluated on a Land (LAND CT2001A) battery test system within a voltage range of 2.0 – 4.0 V. All quantum chemical calculations were performed using the Gaussian 16 program. The geometric structures were optimized, and frequency analyses were subsequently carried out at the B3LYP-D3/6-31G(d,p) level of theory. The absence of imaginary frequencies confirmed that the optimized structures correspond to true minima on the potential energy surface. The solvation effects of dimethylacetamide (DMAc) were accounted for using the polarizable continuum model (PCM). Furthermore, the surface electrostatic potential was visualized and analyzed based on the computed electron density, utilizing the Multiwfn 3.8 software and rendered with VMD.

Electrochemical impedance spectroscopy (EIS) was used to test the bulk resistance (R, Ω) of the devices at room temperature. Ionic conductivity ($\sigma, \text{S/cm}$) could be obtained as follows:

$$\sigma = \frac{l}{AR_S}$$

Where l represented the thickness of the electrolyte film (cm), A represented the area of the electrolyte film (cm^2), and R_S represented the bulk resistance (Ω , tested by EIS).

Transference number is calculated by the following equation:

$$t_+ = \frac{I_s(\Delta V - I_0 R_0)}{I_0(\Delta V - I_s R_s)}$$

Where ΔV is the voltage polarization applied, I_0 and R_0 are the initial current and charge-transfer resistance, respectively, I_s and R_s are the steady state current and charge-transfer resistance, respectively.

Supplementary Method 2. Synthesis of molecules

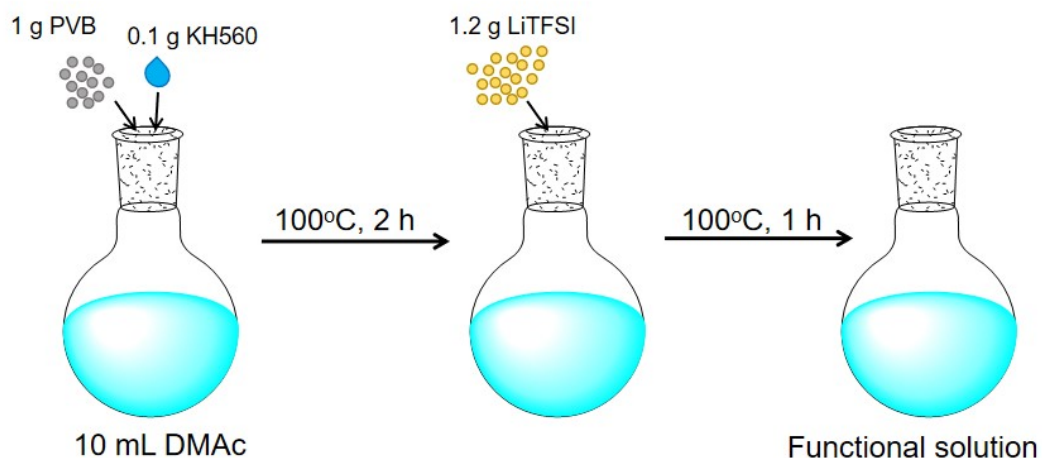
(1) Synthesis of PBDF.

Detailed synthetic process of PBDF was reported in other work.^[8] BDF was dissolved in dimethyl sulfoxide (DMSO) in the presence of 1 mol% Cu(OAc)₂. The solution was heated to

10 °C for 6 h in the air. After that, diluted the solution to 5 mg/mL by DMSO and then dialysis in DMSO. Finally, the dispersion of PBDF in DMSO was obtained.

Supplementary Method 3. Preparation of the solid-state polymer electrolyte (HP-SPE) and electrochromic devices.

(1) Fabrication process of Functional solutions.



In order to obtain an ion transport membranes with excellent comprehensive performance, polyvinyl butyral (PVB) with silane coupling agent (3-Glycidyloxypropyl)trimethoxysilane (KH560) was selected as the polymer matrix with ion-conducting pathways for the high-performance electrolyte membrane owing to its excellent film-forming ability, which provides robust mechanical support, and its high viscosity, which enhances adhesion to the other two functional layers.^[3] A conventional lithium salt, bis(trifluoromethane)sulfonimide lithium salt (LiTFSI), known for its high ionic conductivity, was chosen as the ion conducting component. Firstly, PVB and LiTFSI were dried at 90 °C and 120 °C, respectively, in a vacuum oven for 2 h to get rid of the adsorbed water. Secondly, weighed 1 g dried PVB and 0.1 g KH560 into a reaction bottle and then added 10 mL DMAc into the bottle under N₂ atmosphere. After reacting at 100 °C for 2 h, 1.2 g dried LiTFSI were added into the reaction bottle under N₂ atmosphere. After reacting at 100 °C for 1 h, a colorless, clean, transparent and viscous solution was obtained, which was noted as functional solution.

(2) Fabrication process of high performance solid-state polymer electrolyte (HP-SPE).

Firstly, the functional solution were blade coating (scraper height: 2500 μm) on a 3 μm thick polytetrafluoroethylene film (substrate). Secondly, place the substrate coated with the solution in a vacuum oven at 80 °C for gradient time to detect the residual condition of the solvent. The test results showed that after 48 hours, the solvent residue did not decrease with the increase of time. So set the vacuum drying treatment time to 48 hours. After the vacuum drying treatment was completed, a wet film adhered to the substrate was obtained (C-14%). After the vacuum drying treatment process was completed, C-14% was placed in a device with strong air convection for convection flow drying treatment. The residual solvents in the film were adsorbed by the strong convection air and entered the air from the film. Samples were taken over time for nuclear magnetic resonance testing to detect the residual amount of solvents in the film. Convection flow drying treatment was stopped when the residual amount of solvents did not change over time. The test results showed that after 24 hours, the solvent residue did not decrease with the increase of time. So set the vacuum drying treatment time to 24 hours. As a result, the substrate coated with the solution was placed in a vacuum oven at 80 °C for 48 hours and then placed the substrate covered with the wet film in a device with strong air convection for convection flow drying treatment for 24 hours to get HP-SPE, and the drying process was called ULD.

(3) Fabrication process of the electrochromic layer.

Firstly, weighed 13 mg of 13001 molecules into a clean vial, added 1 mL of THF, and stirred vigorously until the molecules were completely dissolved. Spun coating the solution onto a 2 cm \times 2 cm ITO glass, and then dried it on an 40°C heating table for five minutes to evaporate THF. Finally, a 200 nm thick electrochromic layer was obtained. (note: 13001 molecule is a polymer and can form an independent film.)

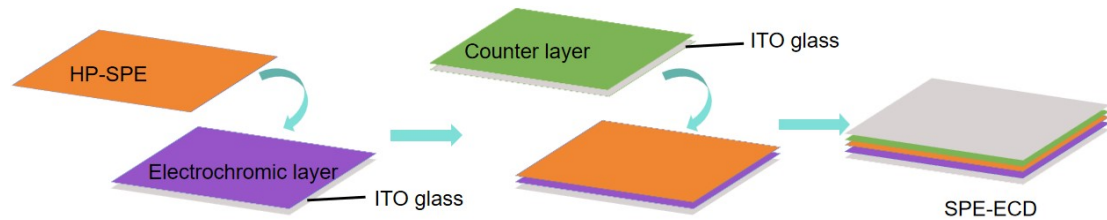
To characterize that the prepared electrochromic layer has no residual solvent, the prepared electrochromic layer was immersed in deuterated DMSO. The polymer film is insoluble in DMSO. After soaking for half an hour, the soaking solution was taken for nuclear magnetic resonance characterization. The results are shown in Figure S11. No characteristic peak of THF appears in the nuclear magnetic resonance spectrum, indicating no residual solvent in the prepared electrochromic layer.

(4) Fabrication process of the counter layer.

Spin coating the dispersion of PBDF in DMSO onto a 2 cm × 2 cm ITO glass, and then vacuum-dried it at 80 °C for one hour to evaporate DMSO. Finally, a 200 nm thick counter layer was obtained.

To characterize that the prepared counter layer has no residual solvent, the prepared counter layer was immersed in CDCl_3 . The polymer film is insoluble in DMSO. After soaking for half an hour, the soaking solution was taken for nuclear magnetic resonance characterization. The results are shown in Figure S10. No characteristic peak of DMSO appears in the nuclear magnetic resonance spectrum, indicating no residual solvent in the prepared counter layer.

(5) Fabrication process of the electrochromic devices (SPE-ECD)

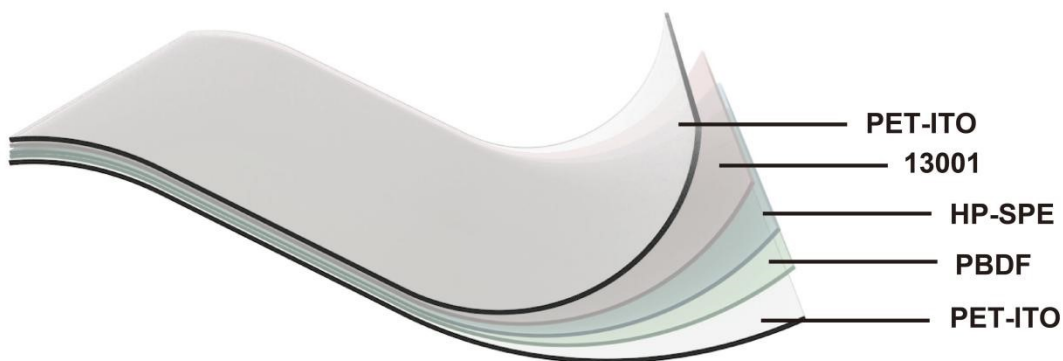


Use scissors to cut the HP-SPE into a rectangular shape of 2 cm × 1 cm. After that, bond the electrochromic layer, the conductive layer and the counter layer in the order shown in the scheme. After that, press hard to make the three functional layers adhere together. Then, the three layers of the device were closely bonded by the hot pressing method (60 °C, 2 hours) to obtain a solid-state device with uniform color change.

(6) Fabrication process of Gel Device. Firstly, 1.4 g PMMA, 0.8 g LiTFSI and 2.5 g PC were weighed in a vial. Then 7 mL acetonitrile was added and stirred vigorously to get *gel electrolyte*. Secondly, blade coating the *gel electrolyte* on the electrochromic layer and standing for 5 minutes to volatilize acetonitrile. Then cover the counter layer onto it to get the gel device.

(7) Fabrication process of the P-C-L Device. Firstly, 2.5 g PEGDA, 8.5 g DMPA, 0.8 g LiTFSI and 2.5 g PC were weighed in a vial and stirred vigorously to get *photopolymerization precursor solution*. Secondly, blade coating the *photopolymerization precursor solution* on the electrochromic layer and then cover the counter layer onto it. Thirdly, irradiate the device with a 5.8 mW/cm² ultraviolet lamp for 5 minutes to get the in-situ polymerization device.

Supplementary Method 4. The shear strength test and load-bearing test of SPE-ECD.



When it comes to **shear strength test and load-bearing test**, for safety concern, glass ITO was replaced with PET-ITO, while other steps remain unchanged (The structural schematic diagram was shown above). Since the HP-SPE interfaced with the 13001 layer and the PBDF layer, the adhesion performance remained unaffected by the change in substrate material.

For shear strength testing of devices with either a conductive layer + electrochromic layer or conductive layer + counter electrode layer, the method is identical. Cover the conductive layer over the respective functional layer (either electrochromic or counter electrode), place a PET-ITO substrate on the opposite side of the conductive layer, then perform extrusion and hot-pressing.

The load-bearing capacity of SPE-ECD was evaluated by placing the device vertically, and a 500 g weight was suspended from it.

Supplementary Method 5. Determination of Solvent Residues by NMR Internal Standard Method

In proton nuclear magnetic resonance (^1H NMR) spectroscopy, for a given proton, its integration is proportional to the molar concentration. Quantitative analysis is performed by comparing the intensities of different absorption peaks and using an internal standard of

known concentration to calibrate the concentration of the unknown sample, thereby calculating the purity of the sample. The calculation formula for the absolute internal standard method is as follows:

$$P_X\% = \frac{I_x \times W_s \times M_x \times N_s \times P_s}{I_s \times W_x \times M_s \times N_x}$$

Where I_x represents the integration value of the signal peak for the analyte, I_s represents the integration value of the signal peak for the internal standard, W_x represents the weighed mass of the analyte sample, typically in milligrams (mg), W_s represents the weighed mass of the internal standard, typically in milligrams (mg), M_x represents the molecular weight of the analyte, M_s represents the molecular weight of the internal standard, N_x represents the number of protons generating the selected integration peak for the analyte, N_s represents the number of protons generating the selected integration peak for the internal standard and P_s represents the purity of the internal standard, expressed as a percentage (%).

In this work, **trimethoxybenzene** was selected as the internal standard.

Supplementary Method 6. Investigation of the effect of air components on DMAc and DMAc-LiTFSI solution.

To investigate the influence of individual air components on neat DMAc, the following experiment was conducted. A 10 mL sample of DMAc was placed in a two-necked round-bottom flask. One neck served as the gas inlet, and the other as the gas outlet. The setup was sealed at all points except for the specified inlet and outlet. Four different gases were separately bubbled through individual DMAc samples under identical conditions: nitrogen (N₂), oxygen (O₂), carbon dioxide (CO₂), and water vapor-saturated nitrogen. The water vapor was introduced by bubbling a stream of N₂ through a water solution before it entered the flask. Each gas was delivered at a

controlled flow rate of 25 mL/min for 60 minutes, resulting in a total gas volume of 1.5 L per experiment.

For investigation of the effect of air components on a DMAc-LiTFSI Solution, a stock solution where the mass ratio of DMAc to LiTFSI was 20:1 was prepared. The experimental gas exposure procedure, as described above, was repeated for these solution aliquots. Each of the four gases (N₂, O₂, CO₂, and water vapor-saturated N₂) was bubbled through one of the vials, with the fifth vial kept as a control without any gas treatment. The same gas flow rate (25 mL/min) and duration (60 min) were strictly maintained.

Supplementary Note 1. Calculation of the Molar Ratio between DMAc and LiTFSI

The molar ratio between DMAc and LiTFSI was determined as follows. The initial mass composition of the system was 1 g of PVB, 0.1 g of KH560, and 1.2 g of LiTFSI. ¹H NMR analysis determined the mass content of residual DMAc in the system to be 5%. This percentage was used to calculate the absolute mass of DMAc using the equation:

$$x / (x + 1 + 0.1 + 1.2) = 0.05$$

where x is the mass of DMAc in grams. Solving this equation gives x = 0.121 g.

With the molecular weights of DMAc (87 g/mol) and LiTFSI (287 g/mol), the molar ratio was calculated as follows:

$$\text{Moles of DMAc} = 0.121 \text{ g} / 87 \text{ g/mol} \approx 0.00139 \text{ mol}$$

$$\text{Moles of LiTFSI} = 1.2 \text{ g} / 287 \text{ g/mol} \approx 0.00418 \text{ mol}$$

$$\text{Molar Ratio (DMAc : LiTFSI)} \approx 0.00139 : 0.00418 \approx 1 : 3$$

Supplementary References

- [1] E. Venezia, P. Salimi, S. Liang, S. Fugattini, L. Carbone and R. P. Zaccaria, *Inorganics*. 2023, **11**, 86.
- [2] T. Chen, H. Wang, Y. Yu, Q. Yan, Z. Wang, J. Yang, L. Li and K. Cui, *Polym. Degrad. Stab.* 2025, **239**, 111373.
- [3] X. Wang, Y. Yang, Q. Jin, Q. Lou, Q. Hu, Z. Xie and W. Song, *Adv. Funct. Mater.* 2023, **33**, 2214417.
- [4] Y. Zhao, X. Chen, S. Tu, X. Zhang, S. Zhang, H. Zhang, X. Zhang and L. Chen, *Opt. Mater.* 2024, **149**, 114991.
- [5] W. Li, X. Zhang, X. Chen, Y. Zhao, L. Wang, M. Chen, J. Zhao, Y. Li and Y. Zhang, *Chem. Eng. J.* 2020, **398**, 125628.
- [6] X. Wu, Z. Bai, B. Bao, Q. Zhang, W. Jiang, Y. Li, C. Hou, K. Li and H. Wang, *Adv. Funct. Mater.* 2023, **34**, 2312358.
- [7] R. Li, F. Lan, L. Tang, Y. Huang, S. Zhao, B. Wang, Y. Han, D. Gao, Q. Jiang, Y. Zhao, Z. Zhao, F. Wang and R. Zhang, *Adv. Funct. Mater.* 2024, **35**, 2419357.
- [8] Z. Ke, A. Abtahi, J. Hwang, K. Chen, J. Chaudhary, I. Song, K. Perera, L. You, K. N. Baustert, K. R. Graham, J. Mei, *J. Am. Chem. Soc.* **2023**, *145*, 3706.